



HAL
open science

FoPen Man-Made Objects Detection with P-band SAR Sub-Aperture Analysis

Thibault Taillade, Elise Colin, Clement Albinet

► **To cite this version:**

Thibault Taillade, Elise Colin, Clement Albinet. FoPen Man-Made Objects Detection with P-band SAR Sub-Aperture Analysis. IEEE IGARSS 2024, Jul 2024, Athènes, Greece. pp.9766-9769, 10.1109/IGARSS53475.2024.10640747 . hal-04718535

HAL Id: hal-04718535

<https://hal.science/hal-04718535v1>

Submitted on 2 Oct 2024

HAL is a multi-disciplinary open access archive for the deposit and dissemination of scientific research documents, whether they are published or not. The documents may come from teaching and research institutions in France or abroad, or from public or private research centers.

L'archive ouverte pluridisciplinaire **HAL**, est destinée au dépôt et à la diffusion de documents scientifiques de niveau recherche, publiés ou non, émanant des établissements d'enseignement et de recherche français ou étrangers, des laboratoires publics ou privés.

FoPen Man-Made Objects Detection with P-band SAR Sub-Aperture Analysis

Thibault Taillade *, Elise Colin[†], Clement Albinet *

* ESRIN, European Space Agency, Italy [†] DTIS-Onera, Palaiseau, France

Abstract—FoPen (Foliage Penetration) SAR systems, especially those operating at low frequencies, are effective for detecting man-made objects in dense forests. This study leverages a single SAR image to distinguish between the strong volume scattering from foliage and the signals of concealed man-made objects, which are typically non-isotropic along the view angle, unlike the azimuthally invariant forest or vegetation. We propose a two-step strategy: firstly, a sliding sublook analysis maintains the azimuthal bandwidth maximally wide for each sublook, producing SAR images with reduced azimuthal resolution but varied central along-track components of the wave-vector, associated with the target’s ‘aspect angle’. Secondly, a homogeneity test—specifically, the coefficient of variation—analyzes the aspect angle dimension of the SAR stack. Preliminary results using P-band datasets from the TropiSAR campaign in Paracou demonstrate the effectiveness of our approach in detecting concealed vehicles and infrastructures.

Index Terms—SAR, FoPen, P-band

I. BACKGROUND AND PURPOSE

Man-made object detection in dense forests presents a significant challenge for security and surveillance applications. Low-frequency FoPen (Foliage Penetration) SAR systems are highly effective for such tasks [1], [2]. The main challenge involves accurately discriminating between the strong volume scattering from foliage and ground-trunk interactions that backscatter towards the radar, and the signals from potential man-made objects concealed below the canopy. The detection of man-made structures in SAR FoPen applications has been explored in [3], [4] by projecting the SAR signal into target and clutter subspaces using a single acquired image. It is also possible to detect ephemeral man-made structures in a FoPen environment using Change Detection (CD) algorithms across two or more SAR images [5], [2], [6].

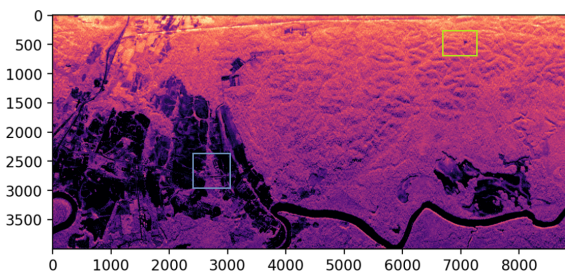
In this contribution, we operate under the condition where only one SAR image of the scene is available. We assume that typical man-made objects exhibit strong backscatter variations as a function of aspect angle, whereas trees or clusters of trees maintain relatively homogeneous backscatter across the same dimension. It is also noteworthy that we prefer low frequencies not only for their natural media penetration capabilities but also because they allow for a wider range of look angles or aspect angles. This aspect is particularly relevant in an airborne context.

Our strategy involves two main steps: the first step entails performing a sliding overlapping sublook analysis while maintaining the azimuthal bandwidth as wide as possible for each sublook, resulting in a set of images with reduced azimuthal

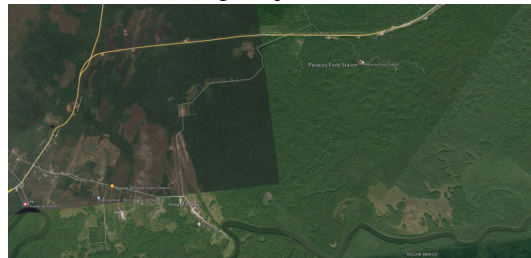
resolution and a varying central along-track component of the wave-vector, referred to as the *aspect angle* dimension. This framework has been utilized for instance in [7] for classification purposes, though with contiguous spectral windows which significantly reduce the resolution achieved. The second step involves conducting a homogeneity test, such as computing the coefficient of variation along the aspect angle dimension. We present some preliminary results of vehicle detection using P-band datasets acquired in Paracou during the TropiSAR campaign.

II. DATASET PRESENTATION:TROPISAR CAMPAIGN

In this study, we use data from TROPISAR campaign that was initially planned in support for BIOMASS mission [6]. During this experiment, some vehicles and a trihedral reflectors have been placed along a small dirt road under foliage on the 24 August 2009 (image tropi402) and acquired with SETHI system for which characteristics are described in Table I.



(a) SAR image acquired on 25/08/09



(b) Optical image of the scene (Google Earth)

Fig. 1: SAR and optical image of the acquired scene

The green and blue boxes in Figure 1 represent ROI that will be used in the paper to provide detailed analysis for man-made object detection.

TABLE I: SETHI characteristics and dataset information for temporal P-band TROPISAR products used for the analysis

Characteristics of Sethi SLC products for TROPISAR	
Polarisation	HH+HV+VH+VV
Range resolution	1.2 m
Azimuth resolution	1.5 m
Central Frequency	400 MHz
wavelength	0.75m
Acquisition dates	From 10 August to 1 September 2009

III. METHODOLOGY

In this section, we present the main steps of the proposed strategy. The first element generates N images using sub-aperture processing. The second step performs a statistical change detection test from these N images, that in our case represent how homogeneous the backscatter of a pixel is, as function of the acquisition aspect angle.

A. Sub-Aperture processing

In order to highlight potential backscatter variability with respect to aspect angle, we compute N sub-aperture images by integrating the signal in the along-track spectral domain K_y^n with varying k_{y0} generating a stack of SAR images backscatter that we denote $s(x, y, k_{y0})$.

$$s(x, y, k_{y0}^n) = \int_{K_x} \int_{K_y^n} a(k_x, k_y) e^{j(k_x x + k_y y)} dk_x dk_y \quad (1)$$

with $k_y = \frac{2f_0}{c} \sin \theta$ and $k_x = \frac{2f_0}{c} \cos \theta$ respectively the wave vectors associated to the along track component (azimuth) and slant range during the acquisition and x, y the range and azimuth coordinates in the slant range plane. In addition, θ that we can consider as an aspect angle between the radar and an object along the acquisition path and f_0 the central radar frequency. The complex backscatter $s(x, y)$ and the spectrum $a(k_x, k_y)$ are related by a 2 dimensional Fourier Transformation. Finally n is the indice corresponding to a given K_y^n spectral domain centered on k_{y0}^n . This procedure generate a stack as shown in Figure 2.

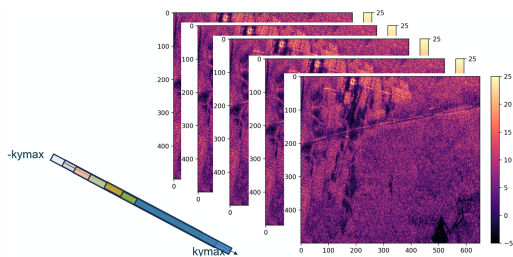


Fig. 2: Generated stack of sub-aperture SAR images with varying k_{y0} with overlapping spectral support

B. Detection of azimuthal backscatter heterogeneity

For man-made objects detection, we favor strategies that keep spatial resolution. The variation coefficient (CV), also

known as relative standard deviation enable to perform such task as we do not require any spatial multilooking. It is mathematically defined in probability theory and statistics by $std(\alpha)/\mu_\alpha$, where $std(\alpha)$ is the standard deviation of the variable α and μ_α its mean value. It can be considered as a normalized measurement of the dispersion of a probability distribution. The CV has been introduced firstly for application in SAR imaging for spatial detection of abrupt changes in [8], [9]. A generation formulation of the variation coefficient derives from the first two statistical moments m_1 (mean) and m_2 (variance) of any distribution :

$$CV = \frac{\sqrt{m_2 - m_1^2}}{m_1} \quad (2)$$

A thorough study can be found in [10] for temporal CV analysis and related statistical properties. In our context, we will not analyze the homogeneity in the temporal direction but in the equivalent aspect angle generated from varying sub-aperture k_{y0} .

IV. RESULTS

In this section is presented preliminary results of the proposed framework using TROPISAR dataset at P-band. The first example shows man-made structures response with clearly identifiable orientation with respect to the sensor path and the second example focuses on objects concealed in the dense canopy.

A. Examples on oriented directional targets

We present in Figure 3 the results of the proposed framework for highly directional man-made objects such fences and buildings using a representation from reactiv framework [10]. The results is an HSV representation that encodes the CV

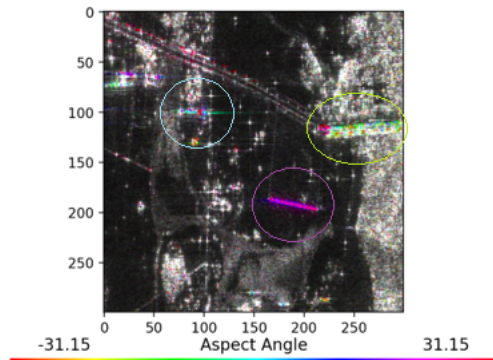


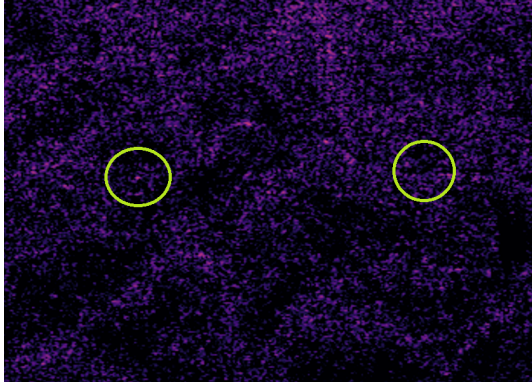
Fig. 3: Example of angular diversity highlighted with reactiv visualization : different orientated man-made structures near agricultural field (blue box in Figure 1). The result are presented with respect to aspect angle θ derived from k_{y0}

and the angle for which the highest change of backscatter is observed and can be interpreted as : 1) dark area are stable with respect to aspect angle with low RCS, 2) white area are stable with respect to aspect angle with high RCS and 3) colored pixel shows an inhomogeneity in the backscatter as function of k_{y0} (i.e aspect angle). In particular this example is interesting

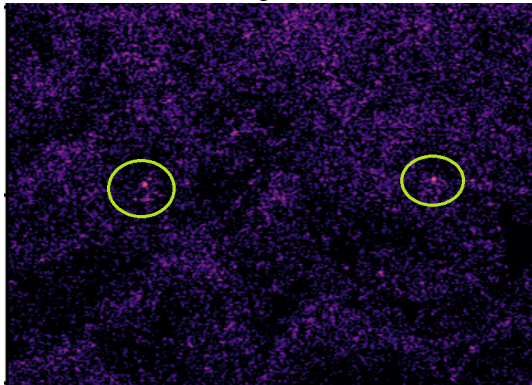
as we can observe three different orientated structures circled respectively in blue, green, and purple. The plane track being in the horizontal direction, we can verify that the blue structure is parallel to the flight track and therefore with a blue signature (zero aspect angle), a green and purple signature shows orientated structures (respectively around -15 degrees and 25 degrees).

B. FoPen man-made objects detection

In this example, we focus on vegetated area of the scene (green box in Figure 1) where target were concealed within the tropical forest during the flight.



(a) Zoom on target area at $\theta = 5^\circ$



(b) Zoom on target area at $\theta = -20^\circ$

Fig. 4: HH SAR images generated with sub-aperture technique. Azimuthal response heterogeneity shown at different sub-aperture equivalent aspect angle **a**. Image with ROI over targets at aspect angle = $\theta = 5^\circ$ (No strong backscattering from the targets), **(b)**. Image with ROI over targets at aspect angle = $\theta = -20^\circ$ (Strong backscattering from the targets)

In Figure 4a and 4b we highlight the backscattering behaviour variability as function of center aspect angle θ used to focus the sub aperture images. The Figure 4a reveals a low backscatter intensity of the targets whereas 4b highlights quite strong backscattering intensity that the targets become visible on naked eye. In addition pictures of detected objects are shown in Figure 5a and Figure 5b.

To go further and obtain an overall diagnostic of the variability we use the variation coefficient and reactiv visualization



(a) Picture of Isuzu from [11]



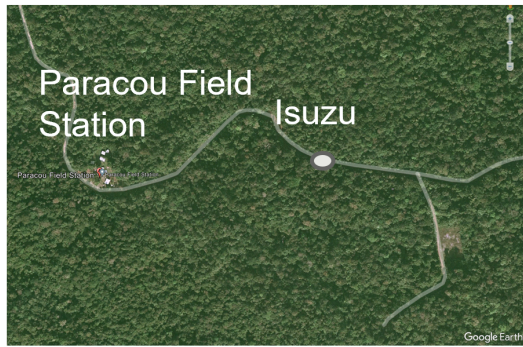
(b) Picture of Paracou research station

Fig. 5: Pictures of concealed vechile and building in tropical forest from [6] **a**. Isuzu concealed **(b)**. Paracou reasearch station)

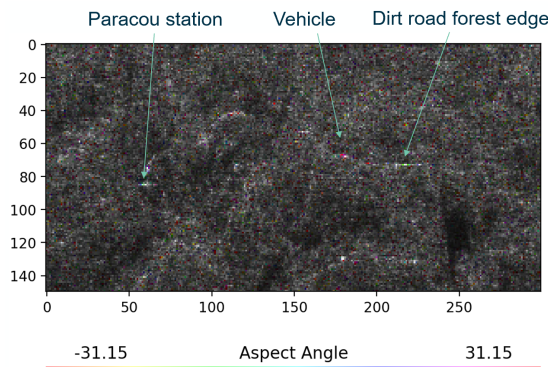
to highlight the pixels for which the azimuthal backscatter is the most inhomogenous. The Figure 6a shows the position of the Isuzu and the Parcou Field Station on an optical image and the Figure 6b reveals with colors both of them. We can also notice a strong signature of a dirt road in green. Finally the Figure 6c shows the very strong backscattering variability in particular for the isuzu that goes from 10dB to -20dB depending on the aspect angle used to re-focus the SAR image. On the contrary the forest remains between 0 and 5 dB of RCS.

V. DISCUSSIONS AND CONCLUSION

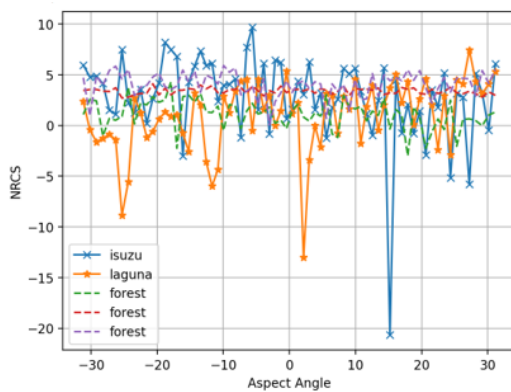
In the context of object detection under vegetation cover, conventional methods typically rely on change detection, which requires the use of multiple images acquired from the site of interest. However, our study has proposed an innovative method that allows for the detection of targets from a single



(a) Optical image and man-made structure locations



(b) Visualization of results using reactiv



(c) Backscattering as function of aspect angle

Fig. 6: Detection of man made objects with P-band sub-aperture analysis. **a.** Optical image and targets locations, **b.** Detection map with highlighted targets, 50 images were generated with full range resolution and half azimuth bandwidth resolution **c.** Plot of backscatter as function of aspect angle for vehicles and forest, blue and yellow curves corresponds to the circled objects (isuzu)

SLC image by studying their anisotropic properties. This approach represents a significant advancement in the field, especially in tropical forest environments where detection is complicated by the dense vegetation.

We have applied a sub-aperture-based framework to identify non-isotropic targets in the FoPen context. The first step describes the strategy of overlapping sub-apertures, while the second step consists of a homogeneity test along the equivalent

aspect angle of the considered sub-aperture. Preliminary studies have revealed promising results, enabling us to identify the Paracou Field station and the Isuzu car in the images thanks to our framework. Dirt roads generated false alarms in detection but can be considered anthropic artifacts.

Further studies will examine the optimal sizing in terms of bandwidth and the number of images needed, as well as the best compromise between the probability of detection and the False Alarms Rate. The integration of the full polarimetric signal could also improve performance.

REFERENCES

- [1] B. Hallberg, G. S. Lars, M. H. Ulander, and P. Frolind, "Individual tree detection using CARABAS-II," in *IGARSS 2003. 2003 IEEE International Geoscience and Remote Sensing Symposium. Proceedings (IEEE Cat. No.03CH37477)*, vol. 3, pp. 1639–1641, 2003.
- [2] L. M. H. Ulander, M. Lundberg, W. Pierson, and A. Gustavsson, "Change detection for low-frequency SAR ground surveillance," *IEEE Proceedings - Radar, Sonar and Navigation*, vol. 152, no. 6, pp. 413–420, 2005.
- [3] R. Durand, G. Ginolhac, L. Thirion-Lefevre, and P. Forster, "Back projection version of subspace detector sar processors," *IEEE Transactions on Aerospace and Electronic Systems*, vol. 47, no. 2, pp. 1489–1497, 2011.
- [4] F. Brigui, G. Ginolhac, L. Thirion-Lefevre, and P. Forster, "New sar target imaging algorithm based on oblique projection for clutter reduction," *IEEE Transactions on Aerospace and Electronic Systems*, vol. 50, no. 2, pp. 1118–1137, 2014.
- [5] L. Novak, "FOPEN change detection experiments using a CARABAS public release data set," in *Algorithms for Synthetic Aperture Radar Imagery XVII* (E. G. Zelnio and F. D. Garber, eds.), vol. 7699, pp. 292 – 301, International Society for Optics and Photonics, SPIE, 2010.
- [6] P. C. Dubois-Fernandez *et al.*, "The tropisar airborne campaign in french guiana: Objectives, description, and observed temporal behavior of the backscatter signal," *IEEE Transactions on Geoscience and Remote Sensing*, vol. 50, no. 8, pp. 3228–3241, 2012.
- [7] L. Ferro-Famil, A. Reigber, E. Pottier, and W.-M. Boerner, "Scene characterization using subaperture polarimetric SAR data," *IEEE Transactions on Geoscience and Remote Sensing*, vol. 41, no. 10, pp. 2264–2276, 2003.
- [8] R. Touzi, A. Lopes, and P. Bousquet, "A statistical and geometrical edge detector for SAR images," *IEEE Transactions on Geoscience and Remote Sensing*, vol. 26, no. 6, pp. 764–773, 1988.
- [9] T. T. Le, A. Atto, E. Trouvé, and J.-M. Nicolas, "Temporal adaptative filtering of SAR image time-series based on the detection of stable and changed areas," in *5th TerraSAR-X / 4th TanDEM-X Science Team Meeting - 2013*, (Oberpfaffenhofen, Germany), p. 4 pages, June 2013.
- [10] E. Colin Koeniguer and J.-M. Nicolas, "Change Detection Based on the Coefficient of Variation in SAR Time-Series of Urban Areas," *Remote Sensing*, vol. 12, p. 2089, Jun 2020.
- [11] H. Oriot, "Change Detection Analysis for Under-Cover Detection in L and UHF Bands," in *ESA Special Publication*, vol. 713 of *ESA Special Publication*, p. 43, Aug. 2013.